

Evidence of the Singly Cabibbo Suppressed decay $\Lambda_c^+ \rightarrow p\pi^0$

M. Ablikim¹, M. N. Achasov^{5,b}, P. Adlarson⁷⁴, X. C. Ai⁸⁰, R. Aliberti³⁵, A. Amoroso^{73A,73C}, M. R. An³⁹, Q. An^{70,57}, Y. Bai⁵⁶, O. Bakina³⁶, I. Balossino^{29A}, Y. Ban^{46,g}, V. Batozskaya^{1,44}, K. Begzsuren³², N. Berger³⁵, M. Berlowski⁴⁴, M. Bertani^{28A}, D. Bettoni^{29A}, F. Bianchi^{73A,73C}, E. Bianco^{73A,73C}, A. Bortone^{73A,73C}, I. Boyko³⁶, R. A. Briere⁶, A. Brueggemann⁶⁷, H. Cai⁷⁵, X. Cai^{1,57}, A. Calcaterra^{28A}, G. F. Cao^{1,62}, N. Cao^{1,62}, S. A. Cetin^{61A}, J. F. Chang^{1,57}, T. T. Chang⁷⁶, W. L. Chang^{1,62}, G. R. Che⁴³, G. Chelkov^{36,a}, C. Chen⁴³, Chao Chen⁵⁴, G. Chen¹, H. S. Chen^{1,62}, M. L. Chen^{1,57,62}, S. J. Chen⁴², S. M. Chen⁶⁰, T. Chen^{1,62}, X. R. Chen^{31,62}, X. T. Chen^{1,62}, Y. B. Chen^{1,57}, Y. Q. Chen³⁴, Z. J. Chen^{25,h}, W. S. Cheng^{73C}, S. K. Choi^{11A}, X. Chu⁴³, G. Cibinetto^{29A}, S. C. Coen⁴, F. Cossio^{73C}, J. Y. Cui⁴⁹, H. L. Dai^{1,57}, J. P. Dai⁷⁸, A. Dbeyssi¹⁸, R. E. de Boer⁴, D. Dedovich³⁶, Z. Y. Deng¹, A. Denig³⁵, I. Denysenko³⁶, M. Destefanis^{73A,73C}, F. De Mori^{73A,73C}, B. Ding^{65,1}, X. X. Ding^{46,g}, Y. Ding⁴⁰, Y. Ding³⁴, J. Dong^{1,57}, L. Y. Dong^{1,62}, M. Y. Dong^{1,57,62}, X. Dong⁷⁵, M. C. Du¹, S. X. Du⁸⁰, Z. H. Duan⁴², P. Egorov^{36,a}, Y. H. Y. Fan⁴⁵, Y. L. Fan⁷⁵, J. Fang^{1,57}, S. S. Fang^{1,62}, W. X. Fang¹, Y. Fang¹, R. Farinelli^{29A}, L. Fava^{73B,73C}, F. Feldbauer⁴, G. Felici^{28A}, C. Q. Feng^{70,57}, J. H. Feng⁵⁸, K. Fischer⁶⁸, M. Fritsch⁴, C. Fritzsche⁶⁷, C. D. Fu¹, J. L. Fu⁶², Y. W. Fu¹, H. Gao⁶², Y. N. Gao^{46,g}, Yang Gao^{70,57}, S. Garbolino^{73C}, I. Garzia^{29A,29B}, P. T. Ge⁷⁵, Z. W. Ge⁴², C. Geng⁵⁸, E. M. Gersabeck⁶⁶, A. Gilman⁶⁸, K. Goetzen¹⁴, L. Gong⁴⁰, W. X. Gong^{1,57}, W. Gradl³⁵, S. Gramigna^{29A,29B}, M. Greco^{73A,73C}, M. H. Gu^{1,57}, C. Y. Guan^{1,62}, Z. L. Guan²², A. Q. Guo^{31,62}, L. B. Guo⁴¹, M. J. Guo⁴⁹, R. P. Guo⁴⁸, Y. P. Guo^{13,f}, A. Guskov^{36,a}, T. T. Han⁴⁹, W. Y. Han³⁹, X. Q. Hao¹⁹, F. A. Harris⁶⁴, K. K. He⁵⁴, K. L. He^{1,62}, F. H. Heinsius⁴, C. H. Heinz³⁵, Y. K. Heng^{1,57,62}, C. Herold⁵⁹, T. Holtmann⁴, P. C. Hong^{13,f}, G. Y. Hou^{1,62}, X. T. Hou^{1,62}, Y. R. Hou⁶², Z. L. Hou¹, H. M. Hu^{1,62}, J. F. Hu^{55,i}, T. Hu^{1,57,62}, Y. Hu¹, G. S. Huang^{70,57}, K. X. Huang⁵⁸, L. Q. Huang^{31,62}, X. T. Huang⁴⁹, Y. P. Huang¹, T. Hussain⁷², N. Hüsken^{27,35}, W. Imoehl²⁷, J. Jackson²⁷, S. Jaeger⁴, S. Janchiv³², J. H. Jeong^{11A}, Q. Ji¹, Q. P. Ji¹⁹, X. B. Ji^{1,62}, X. L. Ji^{1,57}, Y. Y. Ji⁴⁹, X. Q. Jia⁴⁹, Z. K. Jia^{70,57}, H. J. Jiang⁷⁵, P. C. Jiang^{46,g}, S. S. Jiang³⁹, T. J. Jiang¹⁶, X. S. Jiang^{1,57,62}, Y. Jiang^{70,57}, Y. Jiang⁶², J. B. Jiao⁴⁹, Z. Jiao²³, S. Jin⁴², Y. Jin⁶⁵, M. Q. Jing^{1,62}, T. Johansson⁷⁴, X. K. J. S. Kabana³³, N. Kalantar-Nayestanaki⁶³, X. L. Kang¹⁰, X. S. Kang⁴⁰, M. Kavatsyuk⁶³, B. C. Ke⁸⁰, A. Khokkaz⁶⁷, R. Kiuchi¹, R. Kliemt¹⁴, O. B. Kolcu^{61A}, B. Kopf⁴, M. Kuessner⁴, A. Kupsc^{44,74}, W. Kühn³⁷, J. J. Lane⁶⁶, P. Larin¹⁸, A. Lavania²⁶, L. Lavezzi^{73A,73C}, T. T. Lei^{70,57}, Z. H. Lei^{70,57}, H. Leithoff³⁵, M. Lellmann³⁵, T. Lenz³⁵, C. Li⁴³, C. Li⁴⁷, C. H. Li³⁹, Cheng Li^{70,57}, D. M. Li⁸⁰, F. Li^{1,57}, G. Li¹, H. Li^{70,57}, H. B. Li^{1,62}, H. J. Li¹⁹, H. N. Li^{55,i}, Hui Li⁴³, J. R. Li⁶⁰, J. S. Li⁵⁸, J. W. Li⁴⁹, K. L. Li¹⁹, Ke Li¹, L. J. Li^{1,62}, L. K. Li¹, Lei Li³, M. H. Li⁴³, P. R. Li^{38,j,k}, Q. X. Li⁴⁹, S. X. Li¹³, T. Li⁴⁹, W. D. Li^{1,62}, W. G. Li¹, X. H. Li^{70,57}, X. L. Li⁴⁹, Xiaoyu Li^{1,62}, Y. G. Li^{46,g}, Z. J. Li⁵⁸, C. Liang⁴², H. Liang^{70,57}, H. Liang³⁴, H. Liang^{1,62}, Y. F. Liang⁵³, Y. T. Liang^{31,62}, G. R. Liao¹⁵, L. Z. Liao⁴⁹, Y. P. Liao^{1,62}, J. Libby²⁶, A. Limphirat⁵⁹, D. X. Lin^{31,62}, T. Lin¹, B. J. Liu¹, B. X. Liu⁷⁵, C. Liu³⁴, C. X. Liu¹, F. H. Liu⁵², Fang Liu¹, Feng Liu⁷, G. M. Liu^{55,i}, H. Liu^{38,j,k}, H. M. Liu^{1,62}, Huanhuan Liu¹, Huihui Liu²¹, J. B. Liu^{70,57}, J. L. Liu⁷¹, J. Y. Liu^{1,62}, K. Liu¹, K. Liu¹, K. Y. Liu⁴⁰, Ke Liu²², L. Liu^{70,57}, L. C. Liu⁴³, Lu Liu⁴³, M. H. Liu^{13,f}, P. L. Liu¹, Q. Liu⁶², S. B. Liu^{70,57}, T. Liu^{13,f}, W. K. Liu⁴³, W. M. Liu^{70,57}, X. Liu^{38,j,k}, Y. Liu^{38,j,k}, Y. Liu⁸⁰, Y. B. Liu⁴³, Z. A. Liu^{1,57,62}, Z. Q. Liu⁴⁹, X. C. Lou^{1,57,62}, F. X. Lu⁵⁸, H. J. Lu²³, J. G. Lu^{1,57}, X. L. Lu¹, Y. Lu⁸, Y. P. Lu^{1,57}, Z. H. Lu^{1,62}, C. L. Luo⁴¹, M. X. Luo⁷⁹, T. Luo^{13,f}, X. L. Luo^{1,57}, X. R. Lyu⁶², Y. F. Lyu⁴³, F. C. Ma⁴⁰, H. L. Ma¹, J. L. Ma^{1,62}, L. L. Ma⁴⁹, M. M. Ma^{1,62}, Q. M. Ma¹, R. Q. Ma^{1,62}, R. T. Ma⁶², X. Y. Ma^{1,57}, Y. Ma^{46,g}, Y. M. Ma³¹, F. E. Maas¹⁸, M. Maggiora^{73A,73C}, S. Malde⁶⁸, Q. A. Malik⁷², A. Mangoni^{28B}, Y. J. Mao^{46,g}, Z. P. Mao¹, S. Marcello^{73A,73C}, Z. X. Meng⁶⁵, J. G. Messchendorp^{14,63}, G. Mezzadri^{29A}, H. Miao^{1,62}, T. J. Min⁴², R. E. Mitchell²⁷, X. H. Mo^{1,57,62}, N. Yu. Muchnoi^{5,b}, J. Muskalla³⁵, Y. Nefedov³⁶, F. Nerling^{18,d}, I. B. Nikolaev^{5,b}, Z. Ning^{1,57}, S. Nisar^{12,l}, W. D. Niu⁵⁴, Y. Niu⁴⁹, S. L. Olsen⁶², Q. Ouyang^{1,57,62}, S. Pacetti^{28B,28C}, X. Pan⁵⁴, Y. Pan⁵⁶, A. Pathak³⁴, P. Patteri^{28A}, Y. P. Pei^{70,57}, M. Pelizaeus⁴, H. P. Peng^{70,57}, K. Peters^{14,d}, J. L. Ping⁴¹, R. G. Ping^{1,62}, S. Plura³⁵, S. Pogodin³⁶, V. Prasad³³, F. Z. Qi¹, H. Qi^{70,57}, H. R. Qi⁶⁰, M. Qi⁴², T. Y. Qi^{13,f}, S. Qian^{1,57}, W. B. Qian⁶², C. F. Qiao⁶², J. J. Qin⁷¹, L. Q. Qin¹⁵, X. P. Qin^{13,f}, X. S. Qin⁴⁹, Z. H. Qin^{1,57}, J. F. Qiu¹, S. Q. Qu⁶⁰, C. F. Redmer³⁵, K. J. Ren³⁹, A. Rivetti^{73C}, M. Rolo^{73C}, G. Rong^{1,62}, Ch. Rosner¹⁸, S. N. Ruan⁴³, N. Salone⁴⁴, A. Sarantsev^{36,c}, Y. Schelhaas³⁵, K. Schoenning⁷⁴, M. Scodeggio^{29A,29B}, K. Y. Shan^{13,f}, W. Shan²⁴, X. Y. Shan^{70,57}, J. F. Shangguan⁵⁴, L. G. Shao^{1,62}, M. Shao^{70,57}, C. P. Shen^{13,f}, H. F. Shen^{1,62}, W. H. Shen⁶², X. Y. Shen^{1,62}, B. A. Shi⁶², H. C. Shi^{70,57}, J. L. Shi¹³, J. Y. Shi¹, Q. Q. Shi⁵⁴, R. S. Shi^{1,62}, X. Shi^{1,57}, J. J. Song¹⁹, T. Z. Song⁵⁸, W. M. Song^{34,1}, Y. J. Song¹³, Y. X. Song^{46,g}, S. Sosio^{73A,73C}, S. Spataro^{73A,73C}, F. Stieler³⁵, Y. J. Su⁶², G. B. Sun⁷⁵, G. X. Sun¹, H. Sun⁶², H. K. Sun¹, J. F. Sun¹⁹, K. Sun⁶⁰, L. Sun⁷⁵, S. S. Sun^{1,62}, T. Sun^{1,62}, W. Y. Sun³⁴, Y. Sun¹⁰, Y. J. Sun^{70,57}, Y. Z. Sun¹, Z. T. Sun⁴⁹, Y. X. Tan^{70,57}, C. J. Tang⁵³, G. Y. Tang¹, J. Tang⁵⁸, Y. A. Tang⁷⁵, L. Y. Tao⁷¹, Q. T. Tao^{25,h}, M. Tat⁶⁸, J. X. Teng^{70,57}, V. Thoren⁷⁴, W. H. Tian⁵¹, W. H. Tian⁵⁸, Y. Tian^{31,62}, Z. F. Tian⁷⁵, I. Uman^{61B}, S. J. Wang⁴⁹, B. Wang¹, B. L. Wang⁶², Bo Wang^{70,57}, C. W. Wang⁴², D. Y. Wang^{46,g}, F. Wang⁷¹, H. J. Wang^{38,j,k}, H. P. Wang^{1,62}, J. P. Wang⁴⁹, K. Wang^{1,57}, L. L. Wang¹, M. Wang⁴⁹, Meng Wang^{1,62}, S. Wang^{13,f}, S. Wang^{38,j,k}, T. Wang^{13,f}, T. J. Wang⁴³, W. Wang⁵⁸, W. Wang⁷¹, W. P. Wang^{35,18,70,57}, X. Wang^{46,g}, X. F. Wang^{38,j,k}, X. J. Wang³⁹, X. L. Wang^{13,f}, Y. Wang⁶⁰, Y. D. Wang⁴⁵, Y. F. Wang^{1,57,62}, Y. H. Wang⁴⁷, Y. N. Wang⁴⁵, Y. Q. Wang¹, Yaqian Wang^{17,1}, Yi Wang⁶⁰, Z. Wang^{1,57}, Z. L. Wang⁷¹, Z. Y. Wang^{1,62}, Ziyi Wang⁶², D. Wei⁶⁹, D. H. Wei¹⁵, F. Weidner⁶⁷, S. P. Wen¹, C. W. Wenzel⁴, U. Wiedner⁴, G. Wilkinson⁶⁸, M. Wolke⁷⁴, L. Wollenberg⁴, C. Wu³⁹, J. F. Wu^{1,62}, L. H. Wu¹, L. J. Wu^{1,62}, X. Wu^{13,f}, X. H. Wu³⁴, Y. Wu⁷⁰, Y. H. Wu⁵⁴, Y. J. Wu³¹, Z. Wu^{1,57}, L. Xia^{70,57}, X. M. Xian³⁹, T. Xiang^{46,g}, D. Xiao^{38,j,k}, G. Y. Xiao⁴², S. Y. Xiao¹, Y. L. Xiao^{13,f}, Z. J. Xiao⁴¹, C. Xie⁴², X. H. Xie^{46,g}, Y. Xie⁴⁹, Y. G. Xie^{1,57}, Y. H. Xie⁷, Z. P. Xie^{70,57}, T. Y. Xing^{1,62}, C. F. Xu^{1,62}, C. J. Xu⁵⁸, G. F. Xu¹, H. Y. Xu⁶⁵, Q. J. Xu¹⁶, Q. N. Xu³⁰, W. Xu^{1,62}, W. L. Xu⁶⁵, X. P. Xu⁵⁴, Y. C. Xu⁷⁷, Z. P. Xu⁴², Z. S. Xu⁶², F. Yan^{13,f}, L. Yan^{13,f}, W. B. Yan^{70,57}, W. C. Yan⁸⁰, X. Q. Yan¹, H. J. Yang^{50,e}, H. L. Yang³⁴, H. X. Yang¹, Tao Yang¹, Y. Yang^{13,f}, Y. F. Yang⁴³, Y. X. Yang^{1,62}, Yifan Yang^{1,62}, Z. W. Yang^{38,j,k}, Z. P. Yao⁴⁹, M. Ye^{1,57}, M. H. Ye⁹, J. H. Yin¹, Z. Y. You⁵⁸, B. X. Yu^{1,57,62}, C. X. Yu⁴³

G. Yu^{1,62}, J. S. Yu^{25,h}, T. Yu⁷¹, X. D. Yu^{46,g}, C. Z. Yuan^{1,62}, L. Yuan², S. C. Yuan¹, X. Q. Yuan¹, Y. Yuan^{1,62}, Z. Y. Yuan⁵⁸, C. X. Yue³⁹, A. A. Zafar⁷², F. R. Zeng⁴⁹, X. Zeng^{13,f}, Y. Zeng^{25,h}, Y. J. Zeng^{1,62}, X. Y. Zhai³⁴, Y. C. Zhai⁴⁹, Y. H. Zhan⁵⁸, A. Q. Zhang^{1,62}, B. L. Zhang^{1,62}, B. X. Zhang¹, D. H. Zhang⁴³, G. Y. Zhang¹⁹, H. Zhang⁷⁰, H. H. Zhang³⁴, H. H. Zhang⁵⁸, H. Q. Zhang^{1,57,62}, H. Y. Zhang^{1,57}, J. Zhang⁸⁰, J. J. Zhang⁵¹, J. L. Zhang²⁰, J. Q. Zhang⁴¹, J. W. Zhang^{1,57,62}, J. X. Zhang^{38,j,k}, J. Y. Zhang¹, J. Z. Zhang^{1,62}, Jianyu Zhang⁶², Jiawei Zhang^{1,62}, L. M. Zhang⁶⁰, L. Q. Zhang⁵⁸, Lei Zhang⁴², P. Zhang^{1,62}, Q. Y. Zhang^{39,80}, Shuihan Zhang^{1,62}, Shulei Zhang^{25,h}, X. D. Zhang⁴⁵, X. M. Zhang¹, X. Y. Zhang⁴⁹, Xuyan Zhang⁵⁴, Y. Zhang⁷¹, Y. Zhang⁶⁸, Y. T. Zhang⁸⁰, Y. H. Zhang^{1,57}, Yan Zhang^{70,57}, Yao Zhang¹, Z. H. Zhang¹, Z. L. Zhang³⁴, Z. Y. Zhang⁴³, Z. Y. Zhang⁷⁵, G. Zhao¹, J. Zhao³⁹, J. Y. Zhao^{1,62}, J. Z. Zhao^{1,57}, Lei Zhao^{70,57}, Ling Zhao¹, M. G. Zhao⁴³, S. J. Zhao⁸⁰, Y. B. Zhao^{1,57}, Y. X. Zhao^{31,62}, Z. G. Zhao^{70,57}, A. Zhemchugov^{36,a}, B. Zheng⁷¹, J. P. Zheng^{1,57}, W. J. Zheng^{1,62}, Y. H. Zheng⁶², B. Zhong⁴¹, X. Zhong⁵⁸, H. Zhou⁴⁹, L. P. Zhou^{1,62}, X. Zhou⁷⁵, X. K. Zhou⁷, X. R. Zhou^{70,57}, X. Y. Zhou³⁹, Y. Z. Zhou^{13,f}, J. Zhu⁴³, K. Zhu¹, K. J. Zhu^{1,57,62}, L. Zhu³⁴, L. X. Zhu⁶², S. H. Zhu⁶⁹, S. Q. Zhu⁴², T. J. Zhu^{13,f}, W. J. Zhu^{13,f}, Y. C. Zhu^{70,57}, Z. A. Zhu^{1,62}, J. H. Zou¹, J. Zu^{70,57}

(BESIII Collaboration)

¹ *Institute of High Energy Physics, Beijing 100049, People's Republic of China*

² *Beihang University, Beijing 100191, People's Republic of China*

³ *Beijing Institute of Petrochemical Technology, Beijing 102617, People's Republic of China*

⁴ *Bochum Ruhr-University, D-44780 Bochum, Germany*

⁵ *Budker Institute of Nuclear Physics SB RAS (BINP), Novosibirsk 630090, Russia*

⁶ *Carnegie Mellon University, Pittsburgh, Pennsylvania 15213, USA*

⁷ *Central China Normal University, Wuhan 430079, People's Republic of China*

⁸ *Central South University, Changsha 410083, People's Republic of China*

⁹ *China Center of Advanced Science and Technology, Beijing 100190, People's Republic of China*

¹⁰ *China University of Geosciences, Wuhan 430074, People's Republic of China*

¹¹ *Chung-Ang University, Seoul, 06974, Republic of Korea*

¹² *COMSATS University Islamabad, Lahore Campus, Defence Road, Off Raiwind Road, 54000 Lahore, Pakistan*

¹³ *Fudan University, Shanghai 200433, People's Republic of China*

¹⁴ *GSI Helmholtzcentre for Heavy Ion Research GmbH, D-64291 Darmstadt, Germany*

¹⁵ *Guangxi Normal University, Guilin 541004, People's Republic of China*

¹⁶ *Hangzhou Normal University, Hangzhou 310036, People's Republic of China*

¹⁷ *Hebei University, Baoding 071002, People's Republic of China*

¹⁸ *Helmholtz Institute Mainz, Staudinger Weg 18, D-55099 Mainz, Germany*

¹⁹ *Henan Normal University, Xinxiang 453007, People's Republic of China*

²⁰ *Henan University, Kaifeng 475004, People's Republic of China*

²¹ *Henan University of Science and Technology, Luoyang 471003, People's Republic of China*

²² *Henan University of Technology, Zhengzhou 450001, People's Republic of China*

²³ *Huangshan College, Huangshan 245000, People's Republic of China*

²⁴ *Hunan Normal University, Changsha 410081, People's Republic of China*

²⁵ *Hunan University, Changsha 410082, People's Republic of China*

²⁶ *Indian Institute of Technology Madras, Chennai 600036, India*

²⁷ *Indiana University, Bloomington, Indiana 47405, USA*

²⁸ *INFN Laboratori Nazionali di Frascati, (A)INFN Laboratori Nazionali di Frascati, I-00044, Frascati, Italy; (B)INFN*

Sezione di Perugia, I-06100, Perugia, Italy; (C)University of Perugia, I-06100, Perugia, Italy

²⁹ *INFN Sezione di Ferrara, (A)INFN Sezione di Ferrara, I-44122, Ferrara, Italy; (B)University of Ferrara, I-44122, Ferrara, Italy*

³⁰ *Inner Mongolia University, Hohhot 010021, People's Republic of China*

³¹ *Institute of Modern Physics, Lanzhou 730000, People's Republic of China*

³² *Institute of Physics and Technology, Peace Avenue 54B, Ulaanbaatar 13330, Mongolia*

³³ *Instituto de Alta Investigación, Universidad de Tarapacá, Casilla 7D, Arica 1000000, Chile*

³⁴ *Jilin University, Changchun 130012, People's Republic of China*

³⁵ *Johannes Gutenberg University of Mainz, Johann-Joachim-Becher-Weg 45, D-55099 Mainz, Germany*

³⁶ *Joint Institute for Nuclear Research, 141980 Dubna, Moscow region, Russia*

³⁷ *Justus-Liebig-Universität Giessen, II. Physikalisches Institut, Heinrich-Buff-Ring 16, D-35392 Giessen, Germany*

³⁸ *Lanzhou University, Lanzhou 730000, People's Republic of China*

³⁹ *Liaoning Normal University, Dalian 116029, People's Republic of China*

⁴⁰ *Liaoning University, Shenyang 110036, People's Republic of China*

⁴¹ *Nanjing Normal University, Nanjing 210023, People's Republic of China*

⁴² *Nanjing University, Nanjing 210093, People's Republic of China*

⁴³ *Nankai University, Tianjin 300071, People's Republic of China*

⁴⁴ *National Centre for Nuclear Research, Warsaw 02-093, Poland*

⁴⁵ *North China Electric Power University, Beijing 102206, People's Republic of China*

⁴⁶ *Peking University, Beijing 100871, People's Republic of China*

⁴⁷ *Qufu Normal University, Qufu 273165, People's Republic of China*

- ⁴⁸ Shandong Normal University, Jinan 250014, People's Republic of China
- ⁴⁹ Shandong University, Jinan 250100, People's Republic of China
- ⁵⁰ Shanghai Jiao Tong University, Shanghai 200240, People's Republic of China
- ⁵¹ Shanxi Normal University, Linfen 041004, People's Republic of China
- ⁵² Shanxi University, Taiyuan 030006, People's Republic of China
- ⁵³ Sichuan University, Chengdu 610064, People's Republic of China
- ⁵⁴ Soochow University, Suzhou 215006, People's Republic of China
- ⁵⁵ South China Normal University, Guangzhou 510006, People's Republic of China
- ⁵⁶ Southeast University, Nanjing 211100, People's Republic of China
- ⁵⁷ State Key Laboratory of Particle Detection and Electronics, Beijing 100049, Hefei 230026, People's Republic of China
- ⁵⁸ Sun Yat-Sen University, Guangzhou 510275, People's Republic of China
- ⁵⁹ Suranaree University of Technology, University Avenue 111, Nakhon Ratchasima 30000, Thailand
- ⁶⁰ Tsinghua University, Beijing 100084, People's Republic of China
- ⁶¹ Turkish Accelerator Center Particle Factory Group, (A)Istinye University, 34010, Istanbul, Turkey; (B)Near East University, Nicosia, North Cyprus, 99138, Mersin 10, Turkey
- ⁶² University of Chinese Academy of Sciences, Beijing 100049, People's Republic of China
- ⁶³ University of Groningen, NL-9747 AA Groningen, The Netherlands
- ⁶⁴ University of Hawaii, Honolulu, Hawaii 96822, USA
- ⁶⁵ University of Jinan, Jinan 250022, People's Republic of China
- ⁶⁶ University of Manchester, Oxford Road, Manchester, M13 9PL, United Kingdom
- ⁶⁷ University of Muenster, Wilhelm-Klemm-Strasse 9, 48149 Muenster, Germany
- ⁶⁸ University of Oxford, Keble Road, Oxford OX13RH, United Kingdom
- ⁶⁹ University of Science and Technology Liaoning, Anshan 114051, People's Republic of China
- ⁷⁰ University of Science and Technology of China, Hefei 230026, People's Republic of China
- ⁷¹ University of South China, Hengyang 421001, People's Republic of China
- ⁷² University of the Punjab, Lahore-54590, Pakistan
- ⁷³ University of Turin and INFN, (A)University of Turin, I-10125, Turin, Italy; (B)University of Eastern Piedmont, I-15121, Alessandria, Italy; (C)INFN, I-10125, Turin, Italy
- ⁷⁴ Uppsala University, Box 516, SE-75120 Uppsala, Sweden
- ⁷⁵ Wuhan University, Wuhan 430072, People's Republic of China
- ⁷⁶ Xinyang Normal University, Xinyang 464000, People's Republic of China
- ⁷⁷ Yantai University, Yantai 264005, People's Republic of China
- ⁷⁸ Yunnan University, Kunming 650500, People's Republic of China
- ⁷⁹ Zhejiang University, Hangzhou 310027, People's Republic of China
- ⁸⁰ Zhengzhou University, Zhengzhou 450001, People's Republic of China
- ^a Also at the Moscow Institute of Physics and Technology, Moscow 141700, Russia
- ^b Also at the Novosibirsk State University, Novosibirsk, 630090, Russia
- ^c Also at the NRC "Kurchatov Institute", PNPI, 188300, Gatchina, Russia
- ^d Also at Goethe University Frankfurt, 60323 Frankfurt am Main, Germany
- ^e Also at Key Laboratory for Particle Physics, Astrophysics and Cosmology, Ministry of Education; Shanghai Key Laboratory for Particle Physics and Cosmology; Institute of Nuclear and Particle Physics, Shanghai 200240, People's Republic of China
- ^f Also at Key Laboratory of Nuclear Physics and Ion-beam Application (MOE) and Institute of Modern Physics, Fudan University, Shanghai 200443, People's Republic of China
- ^g Also at State Key Laboratory of Nuclear Physics and Technology, Peking University, Beijing 100871, People's Republic of China
- ^h Also at School of Physics and Electronics, Hunan University, Changsha 410082, China
- ⁱ Also at Guangdong Provincial Key Laboratory of Nuclear Science, Institute of Quantum Matter, South China Normal University, Guangzhou 510006, China
- ^j Also at Frontiers Science Center for Rare Isotopes, Lanzhou University, Lanzhou 730000, People's Republic of China
- ^k Also at Lanzhou Center for Theoretical Physics, Lanzhou University, Lanzhou 730000, People's Republic of China
- ^l Also at the Department of Mathematical Sciences, IBA, Karachi 75270, Pakistan

(Dated: November 14, 2023)

Evidence for the singly Cabibbo suppressed decay $\Lambda_c^+ \rightarrow p\pi^0$ is reported for the first time with a statistical significance of 3.7σ based on 6.0 fb^{-1} of e^+e^- collision data collected at center-of-mass energies between 4.600 and 4.843 GeV with the BESIII detector at the BEPCII collider. The absolute branching fraction of $\Lambda_c^+ \rightarrow p\pi^0$ is measured to be $(1.56_{-0.58}^{+0.72} \pm 0.20) \times 10^{-4}$. Combining with the branching fraction of $\Lambda_c^+ \rightarrow n\pi^+$, $(6.6 \pm 1.2 \pm 0.4) \times 10^{-4}$, the ratio of the branching fractions $\Lambda_c^+ \rightarrow n\pi^+$ and $\Lambda_c^+ \rightarrow p\pi^0$ is calculated to be $4.2_{-1.9}^{+2.2}$; this is an important input for the understanding of the decay mechanisms of charmed baryons. In addition, the absolute branching fraction of $\Lambda_c^+ \rightarrow p\eta$ is measured to be $(1.63 \pm 0.31_{\text{stat}} \pm 0.11_{\text{syst}}) \times 10^{-3}$, which is consistent with previous measurements.

Charmed baryon decays provide an excellent system to study the dynamics of light quarks in the environment of a heavy quark. Theoretical interest in hadronic weak decays of the charmed baryon Λ_c^+ has remained strong. However, there is no reliable phenomenological model describing the complicated underlying dynamics of charmed baryon decays. The decay amplitudes of charmed baryons generally consists of factorizable and non-factorizable contributions. Unlike charmed mesons, the non-factorizable contribution is not negligible compared to the factorizable one since the W -exchange process is no longer subject to helicity and color suppression [1, 2]. Studies of non-leptonic weak hadronic decays of Λ_c^+ are therefore essential to understand its decay mechanism. Among them, the singly Cabibbo suppressed (SCS) decays, which receive both the factorizable and non-factorizable contributions, play an important role. However, due to the low decay branching fraction (BF), at the level of $10^{-3} \sim 10^{-4}$ or lower, experimental investigations of Cabibbo suppressed Λ_c^+ decays require higher-statistics data compared to Cabibbo favored Λ_c^+ decays [3–6].

The two-body SCS decays $\Lambda_c^+ \rightarrow p\pi^0$, $\Lambda_c^+ \rightarrow n\pi^+$, and $\Lambda_c^+ \rightarrow p\eta$ are of great importance and have been extensively examined using various phenomenological models [1, 7–14]. These decays contain both non-factorizable W -internal emission and W -exchange processes, which potentially have interference with factorizable components. These studies heavily depend on experimental data as input [15, 16]. Different BFs of these three decays are predicted by various phenomenological models (e.g., the predicted decay BF of $\Lambda_c^+ \rightarrow p\pi^0$ range from 7.5×10^{-5} [1] to 5.7×10^{-4} [9]). Experimental results are needed to distinguish among the different models. Furthermore, the ratio of the BFs between $\Lambda_c^+ \rightarrow n\pi^+$ and $\Lambda_c^+ \rightarrow p\pi^0$ is expected to be less sensitive to the input parameters in the phenomenological models due to the significant cancellation of correlated uncertainties between these two decays. According to SU(3) flavor symmetry, the four-quark operator in the weak transition can be decomposed into the irreducible representations of $\mathcal{O}(6)$ and $\mathcal{O}(15)$. This ratio is predicted to be 2.0 only with $\mathcal{O}(6)$ [9, 11, 14], and 4.7 including the contribution from $\mathcal{O}(6)$ and $\mathcal{O}(15)$ [10]. Other predictions for this ratio are 4.5 or 8.0 from the constituent quark model [7], 3.5 from the dynamical calculation based on the pole model and current algebra [1], and 9.6 from the topological-diagram approach [13]. So, the ratio of the BFs between $\Lambda_c^+ \rightarrow n\pi^+$ and $\Lambda_c^+ \rightarrow p\pi^0$ is also a powerful discriminator between theoretical models.

Experimentally, the decay $\Lambda_c^+ \rightarrow n\pi^+$ was first observed by the BESIII experiment with a BF of $(6.6 \pm 1.2 \pm 0.4) \times 10^{-4}$ [17], and the BF of $\Lambda_c^+ \rightarrow p\eta$ has been precisely measured by the BESIII [18] and Belle [19] experiments. The decay $\Lambda_c^+ \rightarrow p\pi^0$ has, however, not been observed in any experiment previously, with only upper limits on its decay BF being set [18, 19]. By

combining the upper limit of $\mathcal{B}(\Lambda_c^+ \rightarrow p\pi^0) < 8.0 \times 10^{-5}$ from the Belle experiment [19], the ratio of the BFs between $\Lambda_c^+ \rightarrow n\pi^+$ and $\Lambda_c^+ \rightarrow p\pi^0$ is calculated to be greater than 7.2 at the 90% confidence level, which disagrees with most predictions of the phenomenological models [1, 9–11, 14]. There is still no effective explanation for this ratio and experimental results for $\Lambda_c^+ \rightarrow p\pi^0$ are highly desirable.

In this Letter, the first evidence of the SCS decay $\Lambda_c^+ \rightarrow p\pi^0$ is reported using e^+e^- collision data, collected by the BESIII detector at ten center-of-mass (c.m.) energies between 4.600 and 4.843 GeV, corresponding to a total integrated luminosity of 6.0 fb^{-1} [20, 21]. These large data samples collected just above the $\Lambda_c^+\bar{\Lambda}_c^-$ production threshold provide a clean environment and an excellent opportunity to search for $\Lambda_c^+ \rightarrow p\pi^0$ with the double-tag approach. In addition, the decay $\Lambda_c^+ \rightarrow p\eta$ is also measured with the same approach to provide a validation. Throughout this Letter, charge-conjugate modes are implicitly included.

The design and performance of the BESIII detector are described in detail in Ref. [22]. Simulated event samples are produced with a GEANT4-based [23] Monte Carlo (MC) package, which includes the geometric description [24] of the BESIII detector and the detector response. Signal MC samples of $e^+e^- \rightarrow \Lambda_c^+\bar{\Lambda}_c^-$, with $\bar{\Lambda}_c^-$ decaying to nine specific tag modes (as described below and listed in Table I), together with Λ_c^+ decaying to $p\pi^0$ or $p\eta$, are used to determine the detection efficiencies. They are generated by KKMC including the effects of initial-state radiation (ISR) and the beam energy spread. To estimate backgrounds, inclusive MC samples, which consist of $\Lambda_c^+\bar{\Lambda}_c^-$ events, $D_{(s)}^{(*)}$ production, ISR production of vector charmonium(-like) states, Bhabha scattering, $\mu^+\mu^-$, $\tau^+\tau^-$, $\gamma\gamma$ events and other inclusive hadronic processes incorporated in KKMC [25], are generated. Subsequent decays of all intermediate states are modeled with EVTGEN [26, 27] using the BFs either taken from the Particle Data Group [28], when available, or modeled with LUNDCHARM [29, 30]. Final state radiation from charged final state particles is incorporated using the PHOTOS package [31].

This work is carried out by the double-tag (DT) method. First, we select a data sample of the process $e^+e^- \rightarrow \Lambda_c^+\bar{\Lambda}_c^-$, called the single-tag (ST) sample, by tagging a $\bar{\Lambda}_c^-$ baryon with one of the nine exclusive hadronic decay modes, as listed in the first column of Table I. Then, we search for the signal decays $\Lambda_c^+ \rightarrow p\pi^0$ and $\Lambda_c^+ \rightarrow p\eta$ in the system recoiling against the ST $\bar{\Lambda}_c^-$ candidates, referred to as the DT sample hereafter.

Charged tracks, photon candidates as well as the intermediate π^0 , K_S^0 , Λ , and $\bar{\Sigma}^0$ states are selected and reconstructed using the same criteria described in detail in Ref. [17]. In addition, the kaon candidate is now required to have a particle identification (PID) probability to be a kaon greater than 0.0005, in order to suppress

background with pions misidentified as kaons. PID for charged tracks combines measurements of the energy deposited in the MDC, dE/dx , and the flight time from the TOF to form likelihoods $L(h)$ ($h = p, K, \pi$) for each hadron hypothesis. Two variables, the energy difference, $\Delta E = E_{\bar{\Lambda}_c^-} - E_{\text{beam}}$, and the beam energy constrained mass $M_{\text{BC}} = \sqrt{E_{\text{beam}}^2/c^4 - |\vec{p}_{\bar{\Lambda}_c^-}|^2/c^2}$, are adopted to identify the ST $\bar{\Lambda}_c^-$ candidates, where E_{beam} is the beam energy, $E_{\bar{\Lambda}_c^-}$ and $\vec{p}_{\bar{\Lambda}_c^-}$ are the energy and momentum of the $\bar{\Lambda}_c^-$ candidate, respectively. The tagged candidates are selected with the minimum $|\Delta E|$ among all the candidates, and are required to satisfy the ΔE requirements listed in the second column of Table I. To avoid cross feed from the other ST modes, the same requirements as in Ref. [32] are applied for the $\bar{\Lambda}_c^- \rightarrow \bar{p}K_S^0\pi^0$, $\bar{\Lambda}_c^- \rightarrow \bar{p}K_S^0\pi^+\pi^-$ and $\bar{\Lambda}_c^- \rightarrow \bar{p}\pi^+\pi^-$ modes.

The ST yields are extracted by performing unbinned maximum likelihood fits to the corresponding M_{BC} distributions in the range $(2.2, E_{\text{beam}})$ GeV/c^2 . In the fit, the signal shape is modeled by the M_{BC} spectrum extracted from the signal MC sample convolved with a Gaussian function to compensate the resolution difference between the data and the MC simulation. The background is described by an ARGUS function [33] with the endpoint parameter fixed to the corresponding E_{beam} . The fits to the M_{BC} distributions for the nine ST modes are shown in Fig. 1 for the data sample at $\sqrt{s} = 4.682$ GeV; clear $\bar{\Lambda}_c^-$ signals are observed. The detection efficiencies of ST candidates are estimated with MC samples of $e^+e^- \rightarrow \Lambda_c^+\bar{\Lambda}_c^-$ with $\bar{\Lambda}_c^-$ decaying to one of the nine tag modes and Λ_c^+ decaying generically to all possible final states. The ST yields and efficiencies at $\sqrt{s} = 4.682$ GeV are shown in Table I. The results, including the fits, the ST yields and efficiencies, for the other nine c.m. energies are summarized in Supplemental Material [34]. The total ST yield for all the ten c.m. energies is $119398 \pm 413_{\text{stat}}$ events.

TABLE I. The ΔE requirements, the ST yields in data, and the detection efficiencies of the ST and DT candidates for nine tag modes at $\sqrt{s} = 4.682$ GeV. The uncertainties of the ST yields are statistical.

	ΔE (MeV)	N_i^{ST}	ϵ_i^{ST} (%)	ϵ_i^{DT} $p\pi^0$ (%)	ϵ_i^{DT} $p\eta$ (%)
$\bar{p}K^+\pi^-$	(-34, 20)	17557 ± 149	47.03	22.13	20.64
$\bar{p}K_S^0$	(-20, 20)	3486 ± 62	49.61	24.66	22.43
$\bar{p}K^+\pi^-\pi^0$	(-30, 20)	2087 ± 48	41.55	21.00	19.23
$\bar{p}K_S^0\pi^0$	(-30, 20)	4159 ± 100	14.97	7.83	7.12
$\bar{p}K_S^0\pi^+\pi^-$	(-20, 20)	1545 ± 53	17.28	7.73	8.17
$\bar{\Lambda}\pi^-$	(-20, 20)	3776 ± 75	15.36	7.83	7.53
$\bar{\Lambda}\pi^-\pi^0$	(-30, 20)	1352 ± 50	18.21	7.45	7.72
$\bar{\Lambda}\pi^-\pi^+\pi^-$	(-20, 20)	1858 ± 52	12.66	5.14	5.64
$\bar{\Sigma}^0\pi^-$	(-20, 20)	1084 ± 36	20.09	11.48	10.43

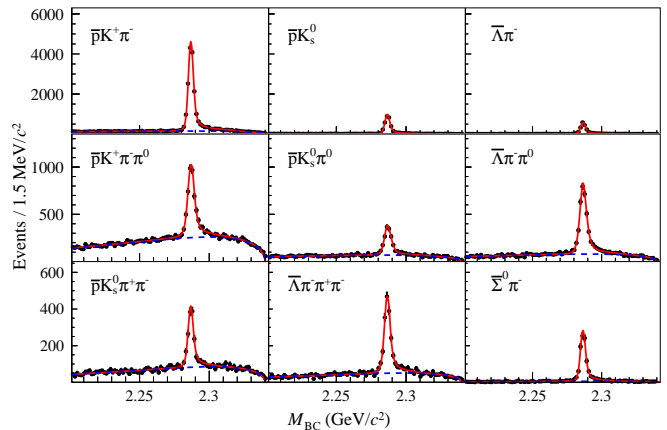


FIG. 1. Fit results for the M_{BC} distributions of the ST modes at $\sqrt{s} = 4.682$ GeV. The points with error bars correspond to the data, the red solid curves are the total fit functions, and the blue dashed curves show the background shapes.

The signal decays $\Lambda_c^+ \rightarrow p\pi^0$ and $\Lambda_c^+ \rightarrow p\eta$ are searched for in the remaining objects recoiling against the ST $\bar{\Lambda}_c^-$ candidates. The selection criteria for charged tracks and photons are the same as those in the ST selection. The distance of the closest approach to the interaction point along the beam direction is required to be less than 10 cm and 20 cm for tight and loose tracks, respectively [17]. In addition, the corresponding distance perpendicular to the beam direction is required to be less than 1 cm for a tight track. To suppress multi-track backgrounds, there must be only one tight track, identified as a proton, and no loose tracks. In order to eliminate noise created by \bar{p} in the electromagnetic calorimeter (EMC), photons are required to be separated from \bar{p} with an opening angle greater than 30° . To improve its purity, the photon candidates are further required to have their lateral moment in the range of (0.05, 0.40) and have an $E_{3 \times 3}/E_{5 \times 5}$ greater than 0.85, where $E_{3 \times 3}$ ($E_{5 \times 5}$) is the shower energy summed over 3×3 (5×5) group of crystals around the central seed crystal. Events with at least two photon candidates are kept for further analysis.

The signal candidate is reconstructed with the selected proton and two photons. For those events with multiple candidates, only the one with the minimum energy difference $|\Delta E_{p2\gamma}| = |E_p + E_{\gamma_1} + E_{\gamma_2} - E_{\text{beam}}|$ is kept, where E_p and $E_{\gamma_{1/2}}$ are the energies of the proton and two photons, respectively. The criterion $-0.080 < \Delta E_{p2\gamma} < 0.035$ GeV, optimized by using the inclusive and signal MC samples, is applied to further suppress the background.

A clear Λ peak is observed in the invariant mass distribution of the proton from the signal side and a π^- from the ST side. Thus, an event is rejected if the invariant mass of any such combination of p and π^- lies within (1.111, 1.121) GeV/c^2 . Similarly, an ω signal is seen in the invariant mass distribution of the π^0 from the

signal side and $\pi^+\pi^-$ pairs from ST side. Events with an invariant mass of any such combination within (0.733, 0.833) GeV/c^2 are also rejected.

The signal decays are examined by $M_{\text{BC}}^{\text{ST}}$ of the tag side, $M_{\gamma\gamma}$ and $M_{\text{BC}}^{p2\gamma}$ of the signal side. Here, $M_{\gamma\gamma}$ is the invariant mass of two photons, and $M_{\text{BC}}^{\text{ST}}$ and $M_{\text{BC}}^{p2\gamma}$ are the beam energy constrained masses of the ST $\bar{\Lambda}_c^-$ and signal candidate. The combined distribution of $M_{\gamma\gamma}$ from the ten c.m. energies is shown in Fig. 2(a), where both π^0 and η signals are observed. The π^0 and η signal regions are defined as (0.115, 0.150) GeV/c^2 and (0.490, 0.583) GeV/c^2 , as indicated by the regions between two magenta and blue lines, respectively. The background in region (0.17, 0.47) GeV/c^2 is dominated by the decays $\Lambda_c^+ \rightarrow \Sigma^+(\rightarrow p\pi^0)\pi^0$ and $\Lambda_c^+ \rightarrow pK_S^0(\rightarrow \pi^0\pi^0)$. The η signal is dominated by $\Lambda_c^+ \rightarrow p\eta$; however, the π^0 signal suffers from a large contamination from inclusive hadronic processes.

The distribution of $M_{\text{BC}}^{\text{ST}}$ versus $M_{\text{BC}}^{p2\gamma}$ and their projections for the candidate events with $M_{\gamma\gamma}$ in the π^0 signal region, are shown in Fig. 2(b) and Fig. 3(a), 3(b), respectively. The events accumulating around the intersection of $M_{\text{BC}}^{\text{ST}} = M_{\Lambda_c}$ and $M_{\text{BC}}^{p2\gamma} = M_{\Lambda_c}$ provide evidence for $\Lambda_c^+ \rightarrow p\pi^0$ (here, M_{Λ_c} denotes the known Λ_c mass [28]). Similarly, Fig. 2(c) and Fig. 3(c), 3(d) illustrate the distribution of $M_{\text{BC}}^{\text{ST}}$ versus $M_{\text{BC}}^{p2\gamma}$ and their projections with $M_{\gamma\gamma}$ in the η signal region, respectively, where the $\Lambda_c^+ \rightarrow p\eta$ signal can be clearly seen. The distribution of inclusive hadronic background MC sample in π^0 signal region is shown in Fig. 2(d), where no accumulation of events in the vicinity of the intersection point is observed. The distribution of the $\Lambda_c^+\bar{\Lambda}_c^-$ background MC sample in the π^0 signal region as well as those in the η signal region are given in the Supplemental Material [34].

The BFs of the decays $\Lambda_c^+ \rightarrow p\eta$ and $\Lambda_c^+ \rightarrow p\pi^0$ are obtained by performing a simultaneous unbinned maximum-likelihood fit on the 2-dimensional (2D) distribution of $M_{\text{BC}}^{p2\gamma}$ versus $M_{\text{BC}}^{\text{ST}}$ among the ten data samples with different c.m. energies. In the fit, the signal is modeled with an MC-simulated shape convolved with Gaussian functions (for $M_{\text{BC}}^{p2\gamma}$ and $M_{\text{BC}}^{\text{ST}}$, individually) representing the resolution difference between data and MC simulation. The mean and width of the Gaussian functions are extracted from the fit to a control sample of $\Lambda_c^+ \rightarrow pK^-\pi^+\pi^0$. The inclusive hadronic background is modeled with the product of two ARGUS functions and a Student's t -distribution describing the dispersion of the inclusive hadronic background in the diagonal direction. Details of the background functions as well as the free and fixed parameters are given in the Supplemental Material [34]. The background from non-signal $e^+e^- \rightarrow \Lambda_c^+\bar{\Lambda}_c^-$ events is modeled with the inclusive MC samples. The same decay BF is shared among the different c.m. energies in the simultaneous fit with the relation

$$\mathcal{B} \cdot \sum_i (\epsilon_i^{\text{DT}} \cdot N_i^{\text{ST}} / \epsilon_i^{\text{ST}}) + N_{\text{bkg}} = N_{\text{total}}, \quad (1)$$

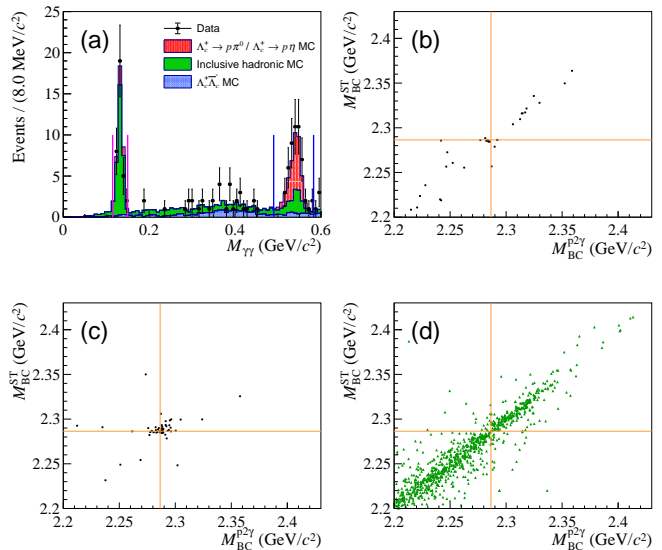


FIG. 2. The invariant mass distribution of $\gamma\gamma$ (a). The scatter plots of $M_{\text{BC}}^{p2\gamma}$ versus $M_{\text{BC}}^{\text{ST}}$ for the candidate events with $M_{\gamma\gamma}$ within (b) π^0 signal region of data, (c) η signal region of data, and (d) π^0 signal region of inclusive hadronic background MC sample. The orange lines denote the nominal Λ_c mass.

where the subscript i represents the i -th ST mode, N_{total} and N_{bkg} denote the total event yields and backgrounds, ϵ_i^{DT} represents the DT detection efficiencies, which are extracted from the DT signal MC samples. The quantities N_i^{ST} , ϵ_i^{ST} and ϵ_i^{DT} used in the 2D fit are summarized in Table I for the data sample with c.m. energy $\sqrt{s} = 4.682$ GeV, and in Supplemental Material [34] for the other nine c.m. energies.

The simultaneous fit yields the BFs $\mathcal{B}(\Lambda_c^+ \rightarrow p\eta) = (1.63 \pm 0.31) \times 10^{-3}$ and $\mathcal{B}(\Lambda_c^+ \rightarrow p\pi^0) = (1.56_{-0.58}^{+0.72}) \times 10^{-4}$, which correspond to the signal yields of 34.7 ± 6.6 and $8.8_{-3.3}^{+4.0}$ events, respectively, for the total ten c.m. energies. The projections of $M_{\text{BC}}^{p2\gamma}$ and $M_{\text{BC}}^{\text{ST}}$ are shown in Fig. 3, where the fit curves describe the data well. The statistical significances, which are estimated from the change of likelihood values and the change of degrees of freedom with and without the signal function included in the fit, are 6.9σ and 3.8σ for $\Lambda_c^+ \rightarrow p\eta$ and $\Lambda_c^+ \rightarrow p\pi^0$, respectively.

The systematic uncertainties for the BF measurement include those associated with the ST and DT yields, the detection efficiencies from the signal side, the BFs of $\pi^0 \rightarrow \gamma\gamma$ and $\eta \rightarrow \gamma\gamma$, and MC statistics.

The uncertainties in the ST detection efficiencies are cancelled by the DT method. The uncertainty associated with DT efficiencies, ϵ_i^{DT} , has several sources. Systematic effects due to the proton tracking and PID efficiencies are estimated using the control sample $J/\psi \rightarrow p\bar{p}\pi^+\pi^-$ [17] and give 1.0% and 1.0%, respectively. The uncertainties originating from the photon reconstruction efficiency and

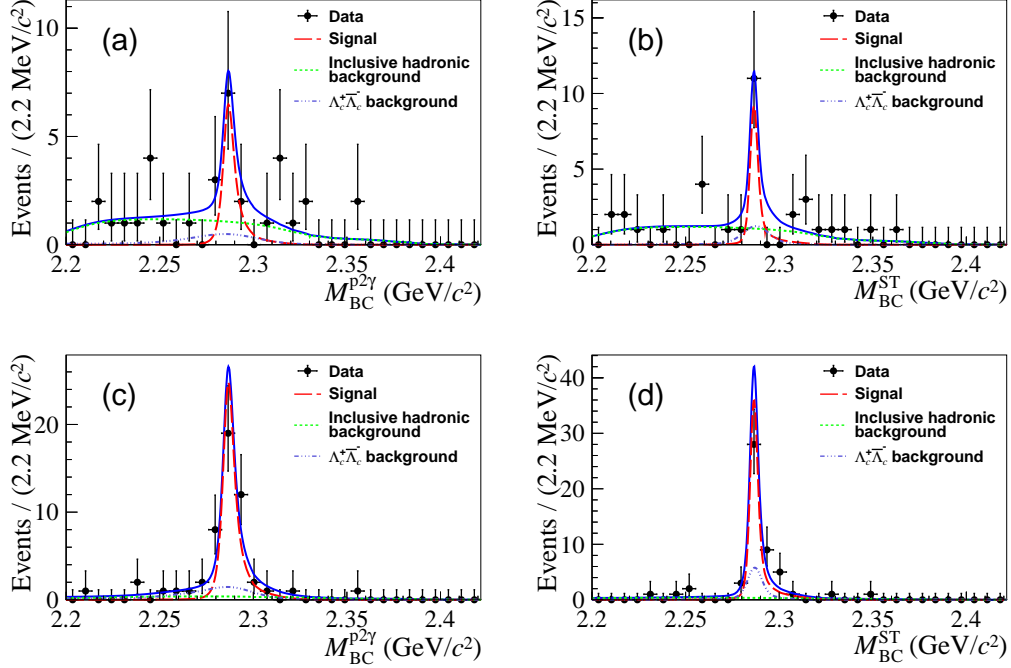


FIG. 3. The 1D projections of the 2D fits for $\Lambda_c^+ \rightarrow p\pi^0$ and $\Lambda_c^+ \rightarrow p\eta$, where (a) and (b) are $M_{BC}^{b2\gamma}$ and M_{BC}^{ST} for $\Lambda_c^+ \rightarrow p\pi^0$, and (c) and (d) are the corresponding plots for $\Lambda_c^+ \rightarrow p\eta$. The black dots denote data and the blue solid curves are the sum of the fit functions. The signal is illustrated by the red dashed curves, while background from the inclusive hadronic events and the non-signal $e^+e^- \rightarrow \Lambda_c^+\bar{\Lambda}_c^-$ events are denoted by the green and blue dashed curves, respectively.

shower shape requirements are studied by the control sample $J/\psi \rightarrow \rho^0\pi^0 \rightarrow \pi^+\pi^-\pi^0$ [35], where 1.0% and 0.5% per photon are obtained, respectively. The uncertainty from the requirement of the opening angle between photon and anti-proton is 0.5% per photon, which is obtained by studying a control sample of $J/\psi \rightarrow p\bar{p}\pi^0$. A Barlow Test [36] is carried out to examine the uncertainties due to the mass window requirements vetoing the backgrounds associated with Λ and ω , where no significant systematic deviation is observed. The systematic uncertainty from the ΔE requirement on the signal side is found to be 0.3% by studying the control samples of modes $\Lambda_c^+ \rightarrow pK^-\pi^+\pi^0$ and $\Lambda_c^+ \rightarrow \Lambda\pi^+\pi^0$. The uncertainty due to the signal MC model is taken as 0.4% [37]. Uncertainties from the BFs of $\eta \rightarrow \gamma\gamma$ and $\pi^0 \rightarrow \gamma\gamma$ are taken from PDG [28]. The uncertainty due to the MC statistics is 0.1%. The ST yields contribute to the uncertainty of BF by 0.5% [17]. The uncertainties due to the DT yields extraction are 5.7% and 12.4% for $\Lambda_c^+ \rightarrow p\eta$ and $\Lambda_c^+ \rightarrow p\pi^0$, respectively, which is the quadratic sum of the individual changes of signal yields obtained from the alternative fits by changing the fixed parameters in the shapes of the signal and background by $\pm 1\sigma$.

Assuming all sources of the uncertainties are uncorrelated, the quadratic sums of the different contributions are taken as the total uncertainties. For $\Lambda_c^+ \rightarrow p\eta$ and $\Lambda_c^+ \rightarrow p\pi^0$, the total systematic uncertainties become 6.4% and 12.8%, respectively. When accounting for

systematic uncertainties in the fit, the significance of the signal for $\Lambda_c^+ \rightarrow p\pi^0$ is 3.7σ .

In summary, based on e^+e^- collision data samples with a total integrated luminosity of 6.0 fb^{-1} collected at c.m. energies between 4.600 and 4.843 GeV with the BESIII detector, the SCS decays $\Lambda_c^+ \rightarrow p\pi^0$ and $\Lambda_c^+ \rightarrow p\eta$ are measured using a DT method. Evidence is obtained for the decay $\Lambda_c^+ \rightarrow p\pi^0$, with a statistical significance of 3.7σ and a decay BF of $(1.56_{-0.58}^{+0.72} \pm 0.20) \times 10^{-4}$. The BF of $\Lambda_c^+ \rightarrow p\eta$ is measured as $(1.63 \pm 0.31_{\text{stat}} \pm 0.11_{\text{syst}}) \times 10^{-3}$, consistent with previous results [18, 19, 37]. The $\mathcal{B}(\Lambda_c^+ \rightarrow p\pi^0)$ result distinctly exceeds the upper limit measured by Belle experiment. Taking $\mathcal{B}(\Lambda_c^+ \rightarrow n\pi^+) = (6.6 \pm 1.2 \pm 0.4) \times 10^{-4}$ [17], the ratio of the BFs between $\Lambda_c^+ \rightarrow n\pi^+$ and $\Lambda_c^+ \rightarrow p\pi^0$ is calculated to be $4.2_{-1.9}^{+2.2}$. This is consistent with various phenomenological predictions [1, 7, 9–11, 13, 14]. The obtained results are important inputs for the validation of different phenomenological models describing the mechanisms of charmed baryon decay.

The BESIII Collaboration thanks the staff of BEPCII, the IHEP computing center and the supercomputing center of the University of Science and Technology of China (USTC) for their strong support. This work is supported in part by National Key R&D Program of China under Contracts Nos. 2020YFA0406400, 2020YFA0406300; National Natural Science Foundation of China (NSFC) under Contracts

Nos. 11335008, 11625523, 12035013, 11705192, 11950410506, 12061131003, 12105276, 12122509, 11635010, 11735014, 11835012, 11935015, 11935016, 11935018, 11961141012, 12022510, 12025502, 12035009, 12192260, 12192261, 12192262, 12192263, 12192264, 12192265, 12221005, 12225509, 12235017, 12005311; China Postdoctoral Science Foundation under Contracts No. 2019M662152, No. 2020T130636; the Fundamental Research Funds for the Central Universities, University of Science and Technology of China under Contract No. WK2030000053; the Chinese Academy of Sciences (CAS) Large-Scale Scientific Facility Program; the CAS Center for Excellence in Particle Physics (CCEPP); Joint Large-Scale Scientific Facility Funds of the NSFC and CAS under Contract No. U1732263, U1832103, U2032111, U1832207; CAS Key Research Program of Frontier Sciences under Contracts Nos. QYZDJ-SSW-SLH003, QYZDJ-SSW-SLH040; 100 Talents Program of CAS; The Institute of Nuclear and Particle Physics

(INPAC) and Shanghai Key Laboratory for Particle Physics and Cosmology; ERC under Contract No. 758462; European Union's Horizon 2020 research and innovation programme under Marie Skłodowska-Curie grant agreement under Contract No. 894790; German Research Foundation DFG under Contracts Nos. 455635585, Collaborative Research Center CRC 1044, FOR5327, GRK 2149; Istituto Nazionale di Fisica Nucleare, Italy; Ministry of Development of Turkey under Contract No. DPT2006K-120470; National Research Foundation of Korea under Contract No. NRF-2022R1A2C1092335; National Science and Technology fund of Mongolia; National Science Research and Innovation Fund (NSRF) via the Program Management Unit for Human Resources & Institutional Development, Research and Innovation of Thailand under Contract No. B16F640076; Polish National Science Centre under Contract No. 2019/35/O/ST2/02907; The Swedish Research Council; U. S. Department of Energy under Contract No. DE-FG02-05ER41374.

-
- [1] H.-Y. Cheng, X.-W. Kang, and F. Xu, *Phys. Rev. D* **97**, 074028 (2018), arXiv:1801.08625 [hep-ph].
- [2] H.-Y. Cheng, *Front. Phys. (Beijing)* **10**, 101406 (2015).
- [3] B. Pal *et al.* (Belle Collaboration), *Phys. Rev. D* **96**, 051102 (2017), arXiv:1707.00089 [hep-ex].
- [4] M. Ablikim *et al.* (BESIII Collaboration), *Chin. Phys. C* **43**, 083002 (2019), arXiv:1811.08028 [hep-ex].
- [5] M. Ablikim *et al.* (BESIII Collaboration), *Phys. Lett. B* **817**, 136327 (2021), arXiv:2012.11106 [hep-ex].
- [6] H.-B. Li and X.-R. Lyu, *Natl. Sci. Rev.* **8**, nwab181 (2021), arXiv:2103.00908 [hep-ex].
- [7] T. Uppal, R. C. Verma, and M. P. Khanna, *Phys. Rev. D* **49**, 3417 (1994).
- [8] S.-L. Chen, X.-H. Guo, X.-Q. Li, and G.-L. Wang, *Commun. Theor. Phys.* **40**, 563 (2003), arXiv:hep-ph/0208006.
- [9] C. Q. Geng, Y. K. Hsiao, C.-W. Liu, and T.-H. Tsai, *Phys. Rev. D* **97**, 073006 (2018), arXiv:1801.03276 [hep-ph].
- [10] C.-Q. Geng, C.-W. Liu, and T.-H. Tsai, *Phys. Lett. B* **790**, 225 (2019), arXiv:1812.08508 [hep-ph].
- [11] C.-D. Lü, W. Wang, and F.-S. Yu, *Phys. Rev. D* **93**, 056008 (2016), arXiv:1601.04241 [hep-ph].
- [12] J. Zou, F. Xu, G. Meng, and H.-Y. Cheng, *Phys. Rev. D* **101**, 014011 (2020), arXiv:1910.13626 [hep-ph].
- [13] H. J. Zhao, Y.-L. Wang, Y. K. Hsiao, and Y. Yu, *JHEP* **02**, 165 (2020), arXiv:1811.07265 [hep-ph].
- [14] K. K. Sharma and R. C. Verma, *Phys. Rev. D* **55**, 7067 (1997), arXiv:hep-ph/9704391.
- [15] L. L. Chau and H. Y. Cheng, *Phys. Rev. Lett.* **56**, 1655 (1986).
- [16] Y. Kohara, *Phys. Rev. D* **44**, 2799 (1991).
- [17] M. Ablikim *et al.* (BESIII Collaboration), *Phys. Rev. Lett.* **128**, 142001 (2022), arXiv:2201.02056 [hep-ex].
- [18] M. Ablikim *et al.* (BESIII Collaboration), *Phys. Rev. D* **95**, 111102 (2017), arXiv:1702.05279 [hep-ex].
- [19] S. X. Li *et al.* (Belle Collaboration), *Phys. Rev. D* **103**, 072004 (2021), arXiv:2102.12226 [hep-ex].
- [20] M. Ablikim *et al.* (BESIII Collaboration), *Chin. Phys. C* **46**, 113002 (2022), arXiv:2203.03133 [hep-ex].
- [21] M. Ablikim *et al.* (BESIII Collaboration), *Chin. Phys. C* **46**, 113003 (2022), arXiv:2205.04809 [hep-ex].
- [22] M. Ablikim *et al.* (BESIII Collaboration), *Nucl. Instrum. Method Phys. Res., Sect. A* **614**, 345 (2010).
- [23] S. Agostinelli *et al.* (GEANT4 Collaboration), *Nucl. Instrum. Method Phys. Res., Sect. A* **506**, 250 (2003).
- [24] K.-X. Huang *et al.*, *NUCL SCI TECH* **33**, 142 (2022), arXiv:2206.10117 [physics.ins-det].
- [25] S. Jadach, B. F. L. Ward, and Z. Was, *Phys. Rev. D* **63**, 113009 (2001).
- [26] D. J. Lange, *Nucl. Instrum. Method Phys. Res., Sect. A* **462**, 152 (2001).
- [27] R. G. Ping, *Chin. Phys. C* **32**, 599 (2008).
- [28] R. L. Workman *et al.* (Particle Data Group), *PTEP* **2022**, 083C01 (2022).
- [29] J. C. Chen, G. S. Huang, X. R. Qi, D. H. Zhang, and Y. S. Zhu, *Phys. Rev. D* **62**, 034003 (2000).
- [30] R.-L. Yang, R.-G. Ping, and H. Chen, *Chin. Phys. Lett.* **31**, 061301 (2014).
- [31] E. Richter-Was, *Phys. Lett. B* **303**, 163 (1993).
- [32] M. Ablikim *et al.* (BESIII Collaboration), *Phys. Rev. Lett.* **120**, 132001 (2018), arXiv:1710.00150 [hep-ex].
- [33] H. Albrecht *et al.* (ARGUS Collaboration), *Phys. Lett. B* **241**, 278 (1990).
- [34] See Supplemental Material for additional details.
- [35] M. Ablikim *et al.* (BESIII Collaboration), *Phys. Rev. D* **81**, 052005 (2010), arXiv:1001.5360 [hep-ex].
- [36] R. Barlow, arXiv:hep-ex/0207026 [hep-ex].
- [37] M. Ablikim *et al.* (BESIII Collaboration), (2023), arXiv:2307.09266 [hep-ex].